crystals

MDPI

Article

Ablation of $BaWO_4$ Crystal by Ultrashort Laser Pulses

Igor Kinyaevskiy [1,*], Pavel Danilov [1], Nikita Smirnov [1], Sergey Kudryashov [1], Andrey Koribut [1], Elizaveta Dunaeva [2], Irina Voronina [2], Yury Andreev [3] and Andrey Ionin [1]

1. P.N. Lebedev Physical Institute of the Russian Academy of Sciences, 119991 Moscow, Russia; pavel-danilov2009@yandex.ru (P.D.); cna1992@mail.ru (N.S.); kudryashovsi@lebedev.ru (S.K.); andrew-koribut@yandex.ru (A.K.); aion@sci.lebedev.ru (A.I.)
2. A.M. Prokhorov General Physics Institute of the Russian Academy of Sciences, 119991 Moscow, Russia; edunaeva@lst.gpi.ru (E.D.); irina.voronina.78@list.ru (I.V.)
3. Institute of Monitoring of Climatic and Ecological Systems of Siberian Branch of Russian Academy of Sciences, 10/2 Academicheskii Ave., 634055 Tomsk, Russia; yuandreev@yandex.ru

* Correspondence: kigor@sci.lebedev.ru

Received: 10 August 2020; Accepted: 26 August 2020; Published: 27 August 2020

check for updates

Abstract: Ablation of $BaWO_4$ Raman crystals with different impurity concentrations by ultrashort laser pulses was experimentally studied. Laser pulses with duration varying from 0.3 ps to 1.6 ps at wavelengths of 515 nm and 1030 nm were applied. A single-pulse optical damage threshold of the crystal surface changed from 1.3 J/cm^2 to 4.2 J/cm^2 depending on the laser pulse parameters and $BaWO_4$ crystal purity. The optical damage threshold under multi-pulse irradiation was an order of magnitude less.

Keywords: $BaWO_4$; optical damage threshold; ablation; ultrashort laser pulse

---

1. Introduction

Stimulated Raman scattering (SRS) is an effective method for different applications of frequency converted technically well-developed lasers. $BaWO_4$ crystal (BWO) with scheelite structure [1] is one of the most efficient crystals for SRS [2,3]. It has a high stationary SRS gain (8.5 cm/GW at the wavelength of 1064 nm) and quite reasonable mechanical (microhardness is 1393–1814 MPa under a load of 0.050 kg [4]), thermal (thermal conductivity is ~2.3 W·m^{-1}·K^{-1} [4]) and optical properties. Growth technology makes it possible to obtain BWO crystals with dimensions of 30 mm in diameter and 110 mm in length with excellent Raman characteristics and reproducible properties [5]. Therefore, a lot of different laser systems have been developed with BWO crystals. For instance, a single-frequency crystalline Raman master oscillator power amplifier (MOPA) system operating at 1178 nm wavelength was demonstrated in [6]. The eye-safe Nd:YVO_4 laser system with intracavity SRS in BWO crystal operating at 1536 nm, which can be used for lidars and in medical applications, was also developed [7].

Progress in ultrafast optics stimulates the active development of SRS lasers and SRS frequency converters for femto- and picosecond laser pulses [8–12], including application of the BWO crystal [11]. For an ultrashort laser pulse with duration shorter than the dephasing time T_2, SRS is in a transient regime, its efficiency sharply decreasing with the pulse shortening [13]. Since a long crystal is inappropriate in ultrafast optics, consequently, to compensate the reduced SRS gain, it is necessary to increase the pump radiation intensity, which is usually limited by the optical damage threshold of the crystal surface. Therefore, in this paper, an ablation of BWO crystals irradiated by ultrashort laser pulses was experimentally studied, and the optical damage threshold for different experimental conditions was determined in fluence and intensity units.

2. Materials and Methods

Our experiments were carried out at the Center for Laser and Nonlinear Optics Technology of the Lebedev Physical Institute of Russian Academy of Science. An optical scheme is shown in Figure 1a. Satsuma femtosecond Yb-fiber laser (Amplitude Systems) operated both at the fundamental frequency (1030 nm wavelength, pulse energy up to 10 μJ) and its second harmonic (515 nm wavelength, pulse energy up to 3.4 μJ). The laser pulse duration was varied from 0.3 ps to 1.6 ps by adjusting an output compressor and was controlled by a scanning interference autocorrelator (AA-20DD, Avesta Project Ltd., pulse duration range 0.01–30 ps). Pulse energy of the TEM_{00} laser mode was smoothly varied by a thin-film reflective attenuator.

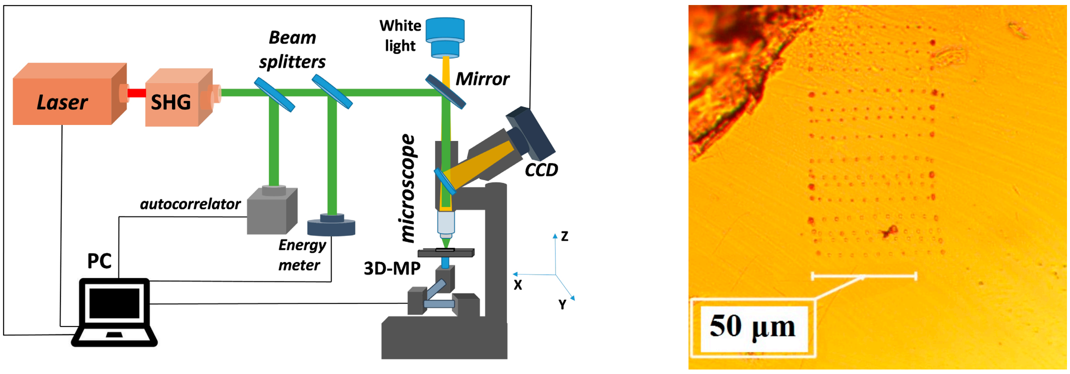

(**a**) (**b**)

Figure 1. (**a**) Experimental setup; (**b**) Series of craters on the $BaWO_4$ (BWO) crystal surface.

BWO crystal ablation was studied by a single-pulse crater method as in [14,15]. Laser radiation was focused on the sample by an optical microscope objective (Bioview 630, Levenhuk) with NA = 0.25. The crystal orientation relative to the laser beam polarization was not controlled. The laser beam radius (at 1/e level) at the crystal surface was ~1.7 μm and ~2.5 μm at wavelengths of 515 nm and 1030 nm, respectively. The laser beam was moved along the crystal surface in such a way that each subsequent pulse irradiated a new place of the crystal surface. Thus, a series of craters (Figure 1b) produced by single laser pulses was obtained. The sizes of the craters produced under various laser pulse energies were measured with an optical microscope. The fluence of optical damage threshold for a beam with a Gaussian intensity profile was calculated by the formula $F_{th} = E_{th}/\pi w_0{}^2$, where E_{th} is the threshold energy under which the ablation takes place when the radiation is focused into a spot with a radius of w_0 (at 1/e level). The values of w_0 and E_{th} were calculated from a linear approximation of the dependence for the square of the crater radius on the logarithm of energy ($R^2 - lnE$).

The BWO crystals were grown at the General Physics Institute of the Russian Academy of Sciences by the Czochralski method from the melting of platinum crucibles in air. For growth, an industrial installation "Crystal-3M" with an automatic control program "Vega" was used. The thermal unit, consisting of a passive platinum screen and zirconium ceramics, provided axial temperature gradients of 90 °C/cm in the growth zone and 5 °C/cm in the annealing zone. The rotation speed was 30 rpm and the pulling rate was varied depending on the boule diameter, so that the volumetric crystallization rate did not exceed 1 cm^3/h.

The initial charge was prepared by solid-phase synthesis from $BaCO_3$ and WO_3 of the high purity grade and then fused into the crucible. For additional purification from impurities the charge was recrystallized once again.

The chemical composition of the grown crystals was monitored by mass spectrometry (Table 1). The analysis was carried out by a device with laser nebulization and ionization of a solid sample. When calculating the total content of uncontrolled impurities, the results of the analysis of B, C, F, Si, P, S, and Cl were not taken into account since the error in their determination in mass spectrometry was very large.

Table 1. Content of main components and impurities in grown crystals of nominally pure barium tungstate.

Crystal Characteristics	Elemental Composition of Crystals, at%			
	Ba	W	O	Impurities
Charge (before recrystallization)	16.61	16.60	66.65	0.10
$BaWO_4$: 1.2 wt% WO_3, colored crystal with scattering centers grown from a charge prepared without recrystallization;	16.62	16.62	66.55	0.09
unpainted crystal with scattering centers	16.61	16.60	66.67	0.07
$BaWO_4$: 1 wt% WO_3, crystal of high optical quality, colorless, grown from a recrystallized charge (upper part);	16.49	16.67	66.49	0.03
The same crystal (lower part)	16.41	16.74	66.54	0.02

It was found that during a long growth process, the evaporation of the more volatile component (WO_3) is observed with violation of the stoichiometry of the melt, which leads to the formation of microscopic scattering centers in the crystal. Therefore, an excess of tungsten oxide was added to the crucible to maintain stoichiometry. The optimal excess for the growth of optically perfect crystals was 1 wt%. The developed technology makes it possible to obtain crystals of high optical quality with a diameter up to 30 mm and a length up to 120 mm. In the experiments, we used two samples of the BWO crystal (Figure 2): "colored" with an impurity concentration of 0.09 at% and "clear" with an impurity concentration of 0.02–0.03 at%. The absorption spectra of these crystals in the wavelength range of 200–1200 nm are shown in Figure 2b. Note that the "colored" crystal with a higher concentration of impurities has a higher absorption.

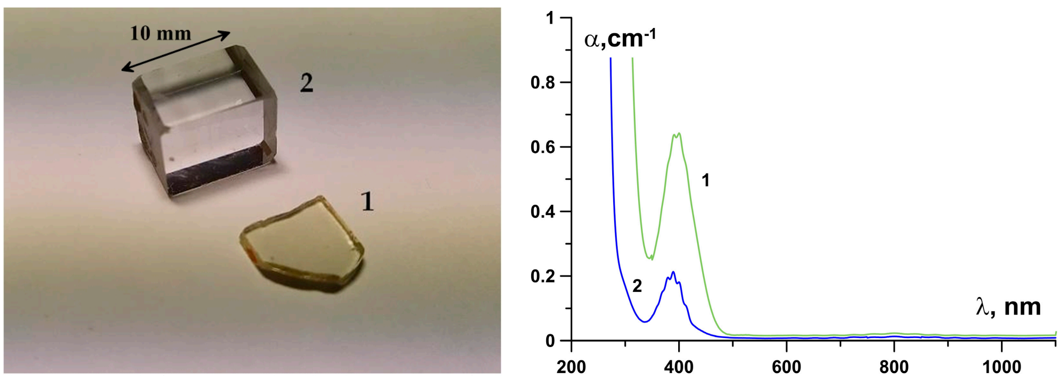

(**a**) (**b**)

Figure 2. (**a**) Crystals appearance; (**b**) absorption coefficient: "1" is for "colored" crystal, "2" is for "clear" crystal.

3. Experimental Results and Discussion

Figure 3 shows the measured optical damage threshold of the BWO crystal surface in fluence and intensity units for laser pulses with 515 nm wavelength and duration from 0.3 ps to 1.6 ps.

For laser pulses at 515 nm and duration of 0.6–1.6 ps, the optical damage fluence of the BWO crystal did not depend on the pulse duration and was equal to 4.2 ± 0.5 J/cm^2, and 3.5 ± 0.5 J/cm^2 for "clear" and "colored" BWO crystal samples, respectively. The slightly higher damage fluence of "clear" crystal was probably due to higher optical quality. When pulse duration was decreased down to 0.3 ps, the optical damage fluence notably fell down for both crystal samples. It was 2.6 ± 0.4 J/cm^2

and 2.2 ± 0.4 J/cm^2 for "clear" and "colored" samples, respectively. This indicates that for shorter pulses with higher intensity (~8 TW/cm^2), significant multiphoton absorption appears which decreases the damage threshold.

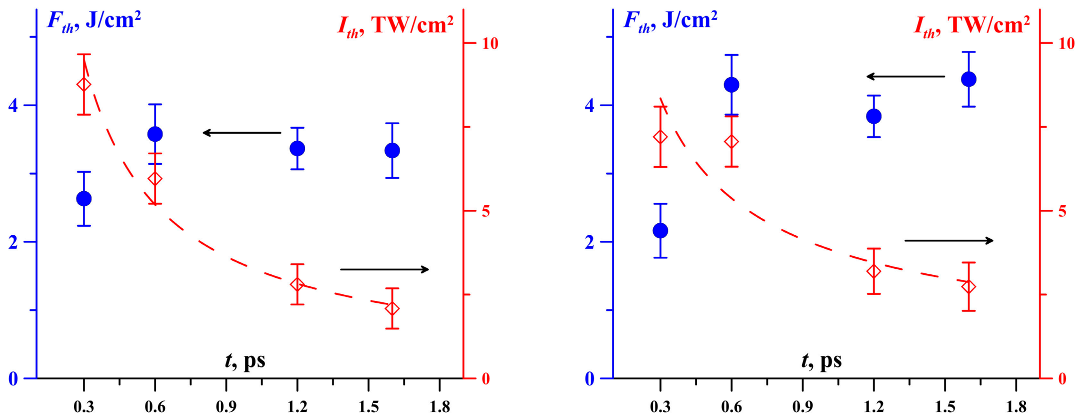

(a) (b)

Figure 3. Dependence of optical damage threshold (fluence and intensity) of BWO crystal surface on the laser pulse duration at 515 nm wavelength for (**a**) "colored" and (**b**) "clear" BWO crystal.

The dependence of the BWO crystal optical damage threshold on pulse duration at the wavelength of 1030 nm was more complicated (Figure 4). For the "colored" sample, the fluence threshold practically did not change and was equal to 1.4 ± 0.4 J/cm^2. For the "clear" sample, the fluence threshold was higher than for the "colored" one and decreased from 3.0 ± 0.4 J/cm^2 down to 1.3 ± 0.3 J/cm^2 with a pulse duration decrease from 1.6 ps down to 0.3 ps. Such a behavior can be associated with nonlinear (multiphoton) absorption. However, it was quite an unexpected result that the optical damage threshold for radiation at 1030 nm was ~2 times lower than for radiation at 515 nm, which cannot be explained by interband absorption (Figure 2b). A possible reason for this fact is an appearance of resonant micro–nano-defects on the surface, which are difficult to register during measuring of the absorption over the entire crystal length. Paper [16] demonstrated that the number of defects on the BWO crystal surface and near-surface layer is significantly higher than in its volume. The presence of defects resonantly absorbing at 1030 nm is indirectly confirmed by the lowest optical damage threshold of the "colored" sample and by appearance of its surface cleavages, which were not observed under the same experimental conditions for the "clear" crystal and for the 515 nm laser pulse.

Table 2 shows a comparison of our results with the results obtained under other experimental conditions. Note, that optical damages of the BWO crystal surface were reported in several papers [11,17–20], but in a number of them, for example in [20], their values were not presented. To complete the data, we also measured the optical damage thresholds of BWO crystals at 1030 nm under the pulse-periodic laser mode (1 KHz pulse repetition rate), under the same conditions as in [11]. The results obtained in this paper are also presented in Table 2 which demonstrates the dependence on optical damage fluence versus pulse duration for picosecond and sub-picosecond pulses to be close to that for nanosecond pulses, i.e., intensity was about three orders of magnitude higher. Moreover, it should be noted that a single pulse damage threshold was one order of magnitude higher than for multi-pulse irradiation. This fact is in accordance with other papers; see, for example, [21].

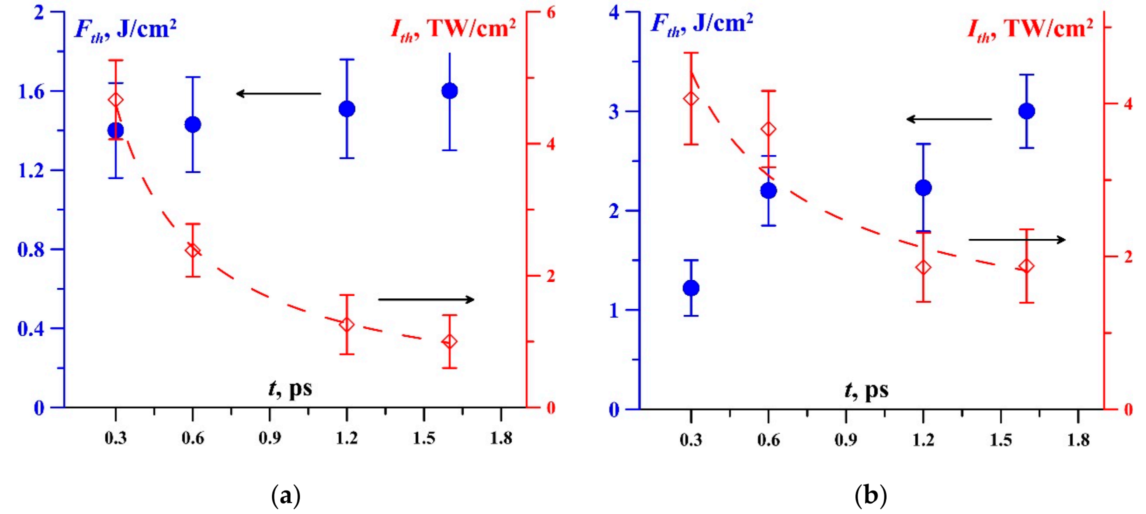

Figure 4. Dependence of optical damage threshold (fluence and intensity) of BWO crystal on the laser pulse duration at 1030 nm wavelength for (**a**) "colored" and (**b**) "clear" BWO crystal.

Table 2. Optical damage threshold of BWO surface at different experimental conditions.

Laser	Wavelength, nm	Repetition Rate, Hz	Pulse Duration, ns	Intensity Threshold, GW/cm^2	Fluence Threshold, J/cm^2	Reference
Nd:YAG	1064	Single pulse	40	0.055	2.2	[17]
N/A	1064	N/A	4.2	2	8	[18]
Second harmonic Ti:Sa laser	472	10	1.1×10^{-4}	2×10^3	0.25	[19]
Second harmonic Yb-fiber	515	10^3	3×10^{-4}	0.8×10^3	0.24	[11]
Yb-fiber	1030	10^3	3×10^{-4}	0.47×10^3	0.14	Current paper
Second harmonic Yb-fiber	515	Single pulse	3×10^{-4}	8.3×10^3	2.6	Current paper
Second harmonic Yb-fiber	515	Single pulse	16×10^{-4}	2.6×10^3	4.2	Current paper
Yb-fiber	1030	Single pulse	3×10^{-4}	4.3×10^3	1.3	Current paper
Yb-fiber	1030	Single pulse	16×10^{-4}	1.9×10^3	3	Current paper

4. Conclusions

An ablation of different quality BWO crystals irradiated by ultrashort laser pulses at 515 nm and 1030 nm with duration varying from 0.3 ps to 1.6 ps was experimentally studied. The optical damage threshold (both fluence and intensity) was measured. The highest damage threshold was recorded for the "clear" crystal sample irradiated by laser pauses at 515 nm and duration of 0.6–1.6 ps. It decreased down to 2.6 ± 0.4 J/cm^2 for a shorter pulse (0.3 ps) due to multiphoton absorption. For the "colored" crystal sample with the higher number of impurities the damage fluence was about 1.5–2 times less. An unexpected result was for the optical damage threshold at 1030 nm to be ~2 times lower than that for radiation at 515 nm. This fact can be associated with resonant surface defects, and it required additional research.

Author Contributions: I.K.: project administration, data processing, visualization, writing; P.D.; experimental investigation; N.S.; experimental investigation and data processing, S.K.; experimental investigation, methodology;

A.K.; experimental investigation and scientific literature investigation; E.D.; BWO crystal grown and preparation; I.V.; BWO crystal grown and preparation; Y.A.; formal analysis, validation and editing; A.I.; conceptualization, writing—review and editing. All authors have read and agreed to the published version of the manuscript.

Funding: This research was supported by the Russian Foundation for Basic Research (RFBR), grant number 20-32-70015 and State Budget Project RAS AAAA-A17-117013050036-3 (Yu.M. Andreev contribution).

Conflicts of Interest: The authors declare no conflict of interest.

References

1. Oliveira, M.C.; Gracia, L.; Nogueira, I.C.; do Carmo Gurgel, M.F.; Mercury, J.M.R.; Longo, E.; Andrés, J. Synthesis and morphological transformation of $BaWO_4$ crystals: Experimental and theoretical insights. *Ceram. Int.* **2016**, *42*, 10913–10921. [CrossRef]
2. Černý, A.; Zverev, P.G.; Jelínková, H.; Basiec, T.T. Efficient Raman shifting of picosecond pulses using $BaWO_4$ crystals. *Opt. Commun.* **2000**, *177*, 397–404. [CrossRef]
3. Černý, A.; Jelínková, H. Near-quantum-limit efficiency of picosecond stimulated Raman scattering in $BaWO_4$ crystal. *Opt. Lett.* **2002**, *27*, 360–362. [CrossRef] [PubMed]
4. Ge, W.W.; Zhang, H.J.; Wang, J.Y.; Liu, J.H.; Xu, X.G.; Hu, X.B.; Jiang, M.H.; Ran, D.G.; Sun, S.Q.; Xia, H.R.; et al. Thermal and mechanical properties of $BaWO_4$ crystal. *J. Appl. Phys.* **2005**, *98*, 013542. [CrossRef]
5. Ivleva, L.I.; Voronina, I.S.; Lykov, P.A.; Brezovskaya, L.Y.; Osiko, V.V. Growth of optically homogeneous $BaWO_4$ single crystals for Raman lasers. *J. Cryst. Growth* **2007**, *304*, 108–113. [CrossRef]
6. Liu, Z.; Rao, H.; Cong, Z.; Xue, F.; Gao, X.; Wang, S.; Tan, W.; Guan, C.; Zhang, X. Single-Frequency $BaWO_4$ Raman MOPA at 1178 nm with 100-ns Pulse Pump. *Crystals* **2019**, *9*, 185. [CrossRef]
7. Zverev, P.G.; Ivleva, L.I. Eye-safe Nd: YVO_4 laser with intracavity SRS in a $BaWO_4$ crystal. *Quantum Electron.* **2012**, *42*, 27–30. [CrossRef]
8. Konyashchenko, A.V.; Losev, L.L.; Pazyuk, V.S. Femtosecond Raman frequency shifter-pulse compressor. *Opt. Lett.* **2019**, *44*, 1646–1649. [CrossRef] [PubMed]
9. Grabtchikov, A.S.; Chulkov, V.A.; Orlovich, V.A.; Schmitt, M.; Maksimenko, R.; Kiefer, W. Observation of Raman conversion for 70-fs pulses in $KGd(WO_4)_2$ crystal in the regime of impulsive stimulated Raman scattering. *Opt. Lett.* **2003**, *28*, 926–928. [CrossRef] [PubMed]
10. Frank, M.; Smetanin, S.N.; Jelínek, M.; Vyhlídal, D.; Kopalkin, A.A.; Shukshin, V.E.; Ivleva, L.I.; Zverev, P.G.; Kubeček, V. Synchronously-pumped all-solid-state $SrMoO_4$ Raman laser generating at combined vibrational Raman modes with 26-fold pulse shortening down to 1.4 ps at 1220 nm. *Opt. Laser Technol.* **2019**, *111*, 129–133. [CrossRef]
11. Kinyaevskiy, I.O.; Kovalev, V.I.; Danilov, P.A.; Smirnov, N.A.; Kudryashov, S.I.; Seleznev, L.V.; Dunaeva, E.E.; Ionin, A.A. Highly efficient stimulated Raman scattering of sub-picosecond laser pulses in $BaWO_4$ for 10.6 µm difference frequency generation. *Opt. Lett.* **2020**, *45*, 2160–2163. [CrossRef] [PubMed]
12. Frank, M.; Smetanin, S.N.; Jelínek, M., Jr.; Vyhlídal, D.; Shukshin, V.E.; Zverev, P.G.; Kubeček, V. 860 fs $GdVO_4$ Raman laser at 1228 nm pumped by 36 ps, 1063 nm laser. *Laser Phys. Lett.* **2019**, *16*, 085401. [CrossRef]
13. Carman, R.L.; Shimizu, F.; Wang, C.S.; Bloembergen, N. Theory of Stokes Pulse Shapes in Transient Stimulated Raman Scattering. *Phys. Rev. A* **1970**, *2*, 60–72. [CrossRef]
14. Zayarny, D.A.; Ionin, A.A.; Kudryashov, S.I.; Makarov, S.V.; Kuchmizhak, A.A.; Vitrik, O.B.; Kulchin, Y.N. Pulse-width-dependent surface ablation of copper and silver by ultrashort laser pulses. *Laser Phys. Lett.* **2016**, *2016 13*, 076101. [CrossRef]
15. Saraeva, I.N.; Kudryashov, S.I.; Rudenko, A.A.; Zhilnikova, M.I.; Ivanov, D.S.; Zayarny, D.A.; Simakin, A.V.; Ionin, A.A.; Garcia, M.E. Effect of fs/ps laser pulsewidth on ablation of metals and silicon in air and liquids, and on their nanoparticle yields. *App. Surf. Sci.* **2019**, *470*, 1018–1034. [CrossRef]
16. Remes, Z.; Bohacek, P.; Nikl, M. Laser profiling of defects in $BaWO_4$ crystals. *Meas. Sci. Technol.* **2012**, *23*, 087001. [CrossRef]
17. Basiev, T.T.; Basieva, M.N.; Gavrilov, A.V.; Ershkov, M.N.; Ivleva, L.I.; Osiko, V.V.; Smetanin, S.N.; Fedin, A.V. Efficient conversion of Nd:YAG laser radiation to eye-safe sperctral region by stimulated Raman scattering in $BaWO_4$ crystal. *Quantum Electron.* **2010**, *40*, 710–715. [CrossRef]

18. Barium and Strontium Tungstate-Molybdate Crystals|EKSMA Optics. Available online: https://eksmaoptics.com/nonlinear-and-laser-crystals/crystals-for-stimulated-raman-scattering/barium-and-strontium-tungstate-molybdate-crystals-for-raman-shift/ (accessed on 26 August 2020).
19. Kinyaevskiy, I.O.; Koribut, A.V.; Grudtsyn, Y.V.; Dunaeva, E.E.; Andreev, Y.M.; Ionin, A.A. Two-color emission of $BaWO_4$ crystals pumped by 472-nm 0.11-ps laser pulses for frequency conversion into the longwave IR domain. *Laser Phys. Lett.* **2020**. accepted.
20. Basiev, T.T.; Basieva, M.N.; Doroshenko, M.E.; Fedorov, V.V.; Osiko, V.V.; Mirov, S.B. Stimulated Raman Scattering in Mid IR Range 2.31-2.75-3.7 µm in a $BaWO_4$ Crystal under 1.9 and 1.56 µm Pumping. *Opt. Soc. Am.* **2006**. [CrossRef]
21. Neuenschwander, B.; Jaeggi, B.; Schmid, M.; Hennig, G. Surface structuring with ultra-short laser pulses: Basics, limitations and needs for high throughput. *Physis. Proc.* **2014**, *56*, 1047–1058. [CrossRef]